

A Terminal Iridium Oxo Complex with a Triplet Ground State

Daniel Delony,^a Markus Kinauer,^a Martin Diefenbach,^b Serhiy Demeshko,^a Christian Würtele,^a Max C. Holthausen^{*[b]} and Sven Schneider^{*[a]}

Abstract: Isolation of a terminal iridium oxo complex with an open-shell ($S = 1$) ground state is reported upon hydrogen atom transfer (HAT) from the respective iridium(II) hydroxide. Electronic structure examinations support large spin delocalization to the oxygen atom. Selected oxo transfer reactions indicate ambiphilic reactivity of the Ir=O moiety. Calorimetric and computational examination of the HAT reveal a $\text{BDFE}_{\text{IrO-H}}$ that is sufficient for hydrogen atom abstraction towards C–H bonds and small contributions from entropy and spin-orbit coupling to the HAT thermochemistry.

Terminal transition metal oxo complexes are proposed as key intermediates in several biological and synthetic oxygenation reactions.^[1] Electron-rich platforms are prevalent due to the occupation of M–O antibonding orbitals that weaken the M–O bond of the oxo-transfer reagent. For example, heavier group 9 catalysts (Rh, Ir) have been utilized in catalytic water oxidation, C–H hydroxylation and related nitrene transfer.^[2,3,4] Accordingly, persistent or even isolable oxo/imido complexes of these metals are particularly rare and only obtained in low coordination numbers ($\text{CN} < 5$), as predicted by the ‘oxo wall’.^[5] Pseudo-tetrahedral geometries are dominating group 9 oxo/imido chemistry (Figure 1).^[6,7,8] Beyond group 9, Milstein’s platinum(IV) pincer oxo complex, a series of nickel imides by Hillhouse and co-workers and a recent palladium(II) imide by Munz and co-workers represent the only well documented examples.^[9,10,11] Both exhibit electronic singlet ground states like the tetrahedral Rh/Ir oxo/imido-complexes.

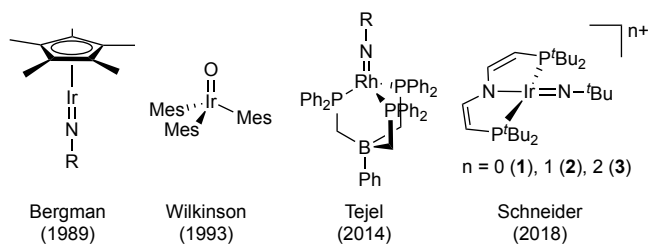
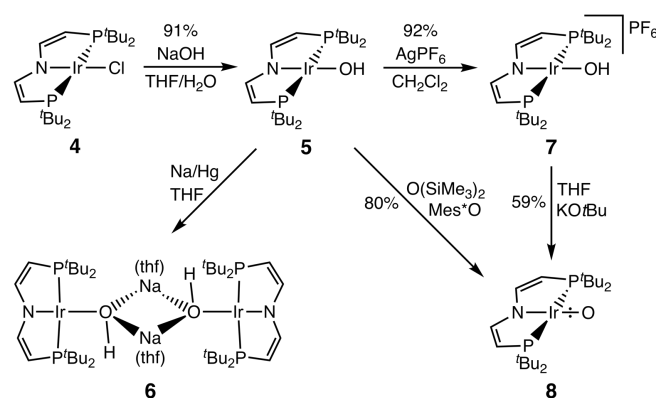


Figure 1. Isolated terminal oxo/imido complexes of rhodium and iridium reported in the literature.

We recently reported a series of terminal iridium(IV/V) nitrido and iridium(III/IV/V) imido complexes, $[\text{Ir}(\text{N})(\text{PNP})]^{n+}$ ($\text{PNP} = \text{N}(\text{CHCHP}^t\text{Bu}_2)_2$; $n = 0, 1$)^[12] and $[\text{Ir}(\text{N}^t\text{Bu})(\text{PNP})]^{n+}$ ($n = 0$ (**1**), **1** (**2**),

2 (**3**); Figure 1).^[13] The neutral imide **1** represents an unprecedented iridium complex with an electronic triplet ground state and high imidyl *N*-radical character, which renders the $\{\text{Ir}(\text{PNP})\}$ -platform attractive to examine electronic effects. In this contribution we report the first isolable, open-shell iridium oxo complex upon hydrogen atom transfer (HAT) from an iridium(II) hydroxo precursor and its reactivity with respect to oxo transfer.



Scheme 1. Syntheses of terminal iridium hydroxo and oxo complexes ($\text{Mes}^*\text{O} = 2,4,6\text{-tris-tertbutylphenoxy}$).

Salt metathesis of $[\text{IrCl}(\text{PNP})]$ (**4**)^[14] with NaOH in THF/ H_2O (2:1) affords the iridium(II) hydroxide complex $[\text{Ir}(\text{OH})(\text{PNP})]$ (**5**) in 91% isolated yield (Scheme 1).^[15] Characterization of **5** by ESI-MS and X-ray crystallography (Figure 2) confirm the formation of a rare, terminal iridium hydroxide complex.^[16] Electrochemical examination in THF by cyclic voltammetry (CV) shows reversible reduction ($E^0 = -2.11$ V; vs. Fc/Fc^+) and oxidation ($E^0 = -0.37$ V) waves on the CV timescale ($\nu = 50\text{--}1000$ $\text{mV}\cdot\text{s}^{-1}$).

Chemical reduction of **5** with Na/Hg at low temperatures (Scheme 1) yields a thermally unstable species, with broadened signals in the diamagnetic NMR region ($\delta_{\text{P}} = 57$ ppm). X-ray crystallographic characterization confirmed the formation of the dimeric, sodium bridged iridium(III) hydroxyl contact ion pair $\{[\text{Na}(\text{thf})\text{Ir}^{\text{III}}(\text{OH})(\text{PNP})]_2\}$ (**6**; Figure 2). In turn, chemical oxidation of **5** with AgPF_6 (1 eq.) affords the cationic complex $[\text{Ir}(\text{OH})(\text{PNP})]\text{PF}_6$ (**7**; Scheme 1) in almost quantitative isolated yield. Complex **7** is stable in solution (THF, CH_2Cl_2) over prolonged time. The diamagnetic iridium(III) complex **7** ($\delta_{\text{P}} = 41.3$ ppm) exhibits a similar NMR signature as 2-electron reduced **6**, except for the drastically downfield shifted OH proton ($\delta_{\text{H}}(\mathbf{6})^{\text{THF}} = -2.06$ ppm; $\delta_{\text{H}}(\mathbf{7})^{\text{CD}_2\text{Cl}_2} = 14.6$ ppm). This shift is associated with considerable Ir–O bond shortening along the iridium(I/II/III) redox series (**6**: 2.1341(16) Å; **5**: 1.988(3) Å; **7**: 1.935(3) Å). The strongly deshielded O–H ^1H NMR signal of **7** is therefore attributed to increased O→Ir π -donation.

With the iridium(II/III) hydroxo redox couple **5/7** in hand, terminal iridium(III) oxo complex $[\text{IrO}(\text{PNP})]$ (**8**) was synthesized by two different routes, i.e. the deprotonation of **7** with KO^tBu (59% yield) and HAT from **5** with 2,4,6-tris-tertbutylphenoxy (Mes^*O ; 80% yield), respectively (Scheme 1). The molecular structure of **8**

[a] D. Delony, Dr. M. Kinauer, Dr. S. Demeshko, Dr. C. Würtele, Prof. Dr. S. Schneider
Universität Göttingen
Institut für Anorganische Chemie
Tammannstr. 4, 37077 Göttingen, Germany
E-mail: sven.schneider@chemie.uni-goettingen.de

[b] Dr. M. Diefenbach, Prof. Dr. M.C. Holthausen
Goethe-Universität Frankfurt
Institut für Anorganische und Analytische Chemie
Max-von-Laue-Str. 7, 60438 Frankfurt am Main, Germany
E-mail: max.holthausen@chemie.uni-frankfurt.de

(Figure 2) exhibits approximate square-planar coordination with an almost linear N–Ir–O axis (173.6°). The Ir–O bond (1.827(4) Å) is considerably shorter compared with hydroxide complexes **5**–**7**, in agreement with increased multiple bonding character. However, the only other structurally characterized iridium oxo complex, i.e. Wilkinson’s closed-shell complex $[\text{Ir}^{\text{VO}}(\text{Mes})_3]$,^[8b] exhibits a shorter Ir–O bond (1.725(9) Å). This comparison suggests a reduced Ir–O bond order for **8** due to an electronic $(yz)^2(z^2)(\pi^*_1)^1(\pi^*_2)^1$ configuration with half-filled Ir–O π^* orbitals, in analogy to the isoelectronic imido complex **1**.^[13] Accordingly, the Ir–O stretching frequency of **8** ($\nu = 743 \text{ cm}^{-1}$), which was assigned by comparison with the ^{18}O labeled isotopologue, is considerably lower than that of $[\text{Ir}^{\text{VO}}(\text{Mes})_3]$ ($\nu = 802 \text{ cm}^{-1}$).^[8b]

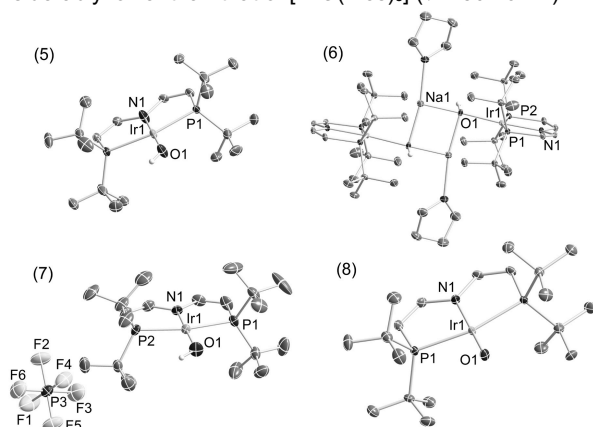


Figure 2. Molecular structures of **5** (top left), **6** (top right), **7** (bottom left) and **8** (bottom right), respectively, derived by single crystal X-ray diffraction. ORTEP plots with anisotropic displacement parameters set at 50% level. Hydrogen atoms (except OH), co-crystallized solvent molecules and disorder of the molecular structure omitted for clarity. Selected bond lengths [Å] and angles [$^\circ$]: **5**: Ir1–O1: 1.988(3), Ir1–N1: 1.988(3), N1–Ir1–O1 180.0. **6**: Ir1–O1: 2.1341(16), Ir1–N1: 2.0352(19), N1–Ir1–O1: 176.53(7). **7**: Ir1–O1 1.935(3), Ir1–N1 1.900(4), N1–Ir1–O1 177.35 (18). **8**: Ir1–O1 1.827(4), Ir1–N1 2.040(4), N1–Ir1–O1 173.6(6).

In analogy to imido complex **1**, three sharp, yet strongly paramagnetically shifted ^1H NMR signals between +21 and –75 ppm in $\text{THF-}d_6$ at r.t. ($\delta_{\text{H}}(\mathbf{1})$: +20 to –60 ppm) and no ^{31}P NMR signal were found. Two of the ^1H NMR signals are almost invariant with temperature over a wide range ($\Delta T = -75$ to +65 $^\circ\text{C}$). The third signal ($\delta_{\text{H}} \approx -75$ ppm) shows approximately linear (Curie) dependence of δ vs. T^{-1} below ca. 250 K with slight bending at higher temperatures. Accordingly, the $\chi_{\text{M}}T$ vs. T curve of a powdered sample, derived by SQUID magnetometry, features temperature independent susceptibility up to around 250 K. The data can be fitted to a spin-Hamiltonian with $S = 1$, $g_{\text{av}} = 2.32$ and large axial zero-field splitting ($D = 647 \text{ cm}^{-1}$).^[17]

As for imide **1**, the magnetic properties in solution and the solid state support an electronic triplet state that is strongly split by spin-orbit coupling (SOC). An energetically isolated ground state results with large temperature independent paramagnetism (TIP) that is 647 cm^{-1} below excited spin-orbit states. Comparison, of **1** ($D(\mathbf{1}) = +466 \text{ cm}^{-1}$)^[12] and **8** reveals larger splitting of the spin-eigenstates for the oxo complex. Within a simple ligand-field picture, this can be attributed to reduced Ir=E (E = NR, O) covalency for the oxo complex leading to a smaller relativistic nephelauxetic effect that reduces the spin-orbit coupling parameter ζ_{eff} with respect to the free ion value.^[18]

This interpretation is corroborated by detailed analysis of the electronic structure. DFT (B3LYP(V)-D3/def2TZVP) reproduces for the $^3\text{A}''$ spin state the short Ir–O bond (1.80 Å) and near linearity of the N–Ir–O angle (179.0°). In contrast, the lowest singlet state exhibits considerable deviation from linearity (157.0°), as also found computationally for a related, isoelectronic singlet Pt^{IV} pincer oxo complex.^[9] The computed triplet ground state of **8** is separated from the singlet by a significant adiabatic energy gap of 41 kJ mol^{-1} .^[19] The SOMOs of **8** exhibit predominant Ir–O π^* character resulting in equal spin density distribution over the iridium and oxygen atom (Figure 3c).

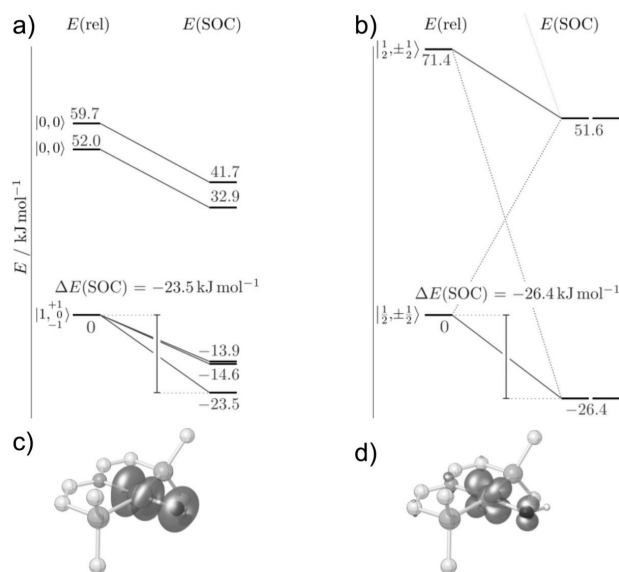
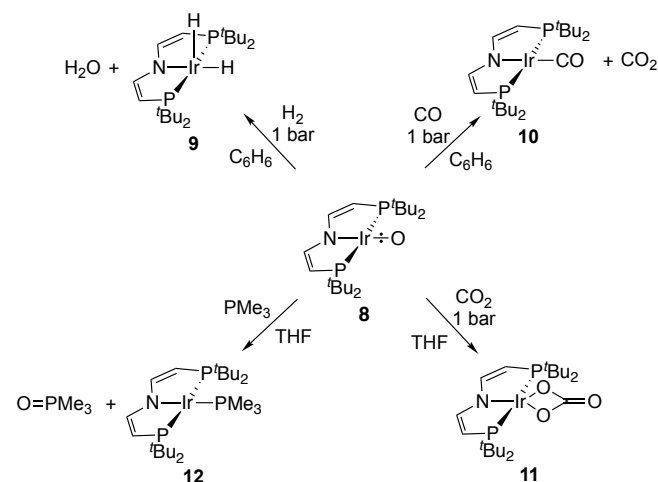


Figure 3. Top: *Ab initio* state correlation diagrams without and with spin-orbit coupling for oxo complex **8** (a) and hydroxo complex **5** (b). Bottom: DFT spin density plots (isovalue 0.0075 a_0^{-3}) for the $^3\text{A}''$ ground state of oxo complex **8** (c) and the ^2A ground state of hydroxo complex **5** (d).

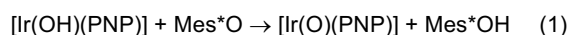
This picture was further refined by multireference calculations using quasi-degenerate perturbation theory (QDPT) to correct for spin-orbit contributions. The scalar-relativistic NEVPT2 computation confirms the $S = 1$ ground state with a vertical excitation energy of 52 kJ mol^{-1} to the lowest singlet state (Figure 3a). SOC stabilizes the lowest spin-free state by 24 kJ mol^{-1} and splits the triplet root into a ground state that is 744 cm^{-1} below two almost degenerate states. The computed axial zero-field splitting parameter ($D_{\text{QDPT}} = 775 \text{ cm}^{-1}$) is in good agreement with the experimentally determined value. The same picture evolved for imide complex **1**, yet with a smaller energetic separation of the spin-orbit ground state (450 cm^{-1}).^[13] supporting the covalency arguments discussed above to rationalize the magnetic properties. The electronic structure analysis indicates that **8** represents an unprecedented iridium oxo biradical complex with strong O-radical character. Its reactivity towards oxo transfer and proton coupled electron transfer (PCET) was probed with selected reagents (Scheme 2). Hydrogenolysis with 1 bar H_2 selectively gives the dihydride complex $[\text{IrH}_2(\text{PNP})]$ (**9**) and water. With CO (1 bar) and PMe_3 (2 eq), the iridium(I) carbonyl and phosphine complexes $[\text{IrL}(\text{PNP})]$ (L = CO (**10**), PMe_3 (**11**))^[20] are formed, respectively, with concomitant release of CO_2 and OPMe_3 . From the reaction with CO_2 (1 bar), the carbonate complex $[\text{Ir}(\text{CO}_3)(\text{PNP})]$ (**12**) could be isolated in over 70 % yield. The

reactions with CO/PMe₃ and CO₂, respectively, indicate ambiphilic reactivity of the oxo moiety.



Scheme 2. Reactivity of oxo complex **8** with selected substrates.

The stability of the oxo/hydroxo HAT couple **8/5** offers experimental access to the O–H bond dissociation (free) energy (BD(F)E). The low selectivity for deprotonation of **7** with a variety of bases precluded BD(F)E derivation via a thermochemical cycle. Instead, the BD(F)E was directly derived by isothermal titration calorimetry (ITC) in THF using Mes^{*}O as HAT titration reagent (eq. 1).^[21]



The slightly exothermic ($\Delta_r H^{\circ}_{\text{HAT}} = -3.83 \pm 0.05 \text{ kJ}\cdot\text{mol}^{-1}$) and endergonic ($\Delta_r G^{\circ}_{\text{HAT}} = +0.0162 \pm 0.087 \text{ kJ}\cdot\text{mol}^{-1}$) reaction allowed for estimating $\text{BDE}_{\text{Ir-O-H}}^{\text{THF}}(\mathbf{5}) = 350 \pm 2 \text{ kJ}\cdot\text{mol}^{-1}$ and $\text{BDFE}_{\text{Ir-O-H}}^{\text{THF}}(\mathbf{5}) = 325 \pm 6 \text{ kJ}\cdot\text{mol}^{-1}$,^[15] i.e. slightly lower than for recently reported cobalt(III) hydroxo complex $[\text{Co}(\text{OH})\{\text{Phb}(\text{tBulm})_3\}]$ ($\text{BDFE}_{\text{Co-O-H}}^{\text{MeCN}} = 354 \text{ kJ}\cdot\text{mol}^{-1}$).^[6f,g] The reaction entropy for equation 1 ($\Delta_r S^{\circ}_{\text{HAT}} = -13 \pm 18 \text{ J}\cdot\text{mol}^{-1}\cdot\text{K}^{-1}$) is in line with small contributions from both the HAT reagent ($S^{\circ}_{\text{Mes}^*\text{O}} \approx S^{\circ}_{\text{Mes}^*\text{OH}}$) and the hydroxo/oxo couple **5/8**.^[22] Minor changes in vibrational and electronic entropies can be expected for 5d metal complexes with energetically well-separated electronic ground states, such as **5** and **8** (Figure 3a/b).^[23]

Explicitly correlated coupled-cluster computations including spin-orbit coupling and solvent effects give an IrO–H BDE of $342 \text{ kJ}\cdot\text{mol}^{-1}$, in excellent agreement with experiment. In view of the large SOC-induced stabilization of **8** (Figure 3a) the contribution to the HAT reaction is of interest. The thermochemistry of bare, heavy metal ions can be largely governed by SOC.^[24] However, sufficient quenching by the ligand field is generally assumed for coordination compounds.^[25] In fact, a differential SOC contribution of less than $3 \text{ kJ}\cdot\text{mol}^{-1}$ ($\Delta\Delta E^{\text{SOC}} = -254 \text{ cm}^{-1}$) was computed for the ground states of **5** and **8** (Figure 3a/b). In a simplified picture, the triplet oxo complex **8** features two ferromagnetically coupled local spins – one Ir- and one O-centered, respectively (Figure 3c). Formation of doublet **5** by HAT quenches the O-centered spin (Figure 3d) whereas the Ir-centered spin is retained. We thus attribute the small net SOC effect to essentially unchanged local Ir spin populations in the hydroxo and the oxo complexes rather than to SOC quenching by the ligand field.

In summary, a terminal iridium oxo complex was obtained by HAT from an iridium(II) hydroxide. Its unprecedented triplet ground state features an equal distribution of the two unpaired electrons between Ir and O and therefore large oxygen-centered radical character. Although SOC strongly influences the ground states of **5** and **8**, it has a negligible effect on the hydroxo/oxo HAT thermochemistry. The oxo complex exhibits ambiphilic reactivity and the IrO–H BDFE ($325 \pm 6 \text{ kJ}\cdot\text{mol}^{-1}$) indicates its suitability for the activation of strong bonds, which will be examined in future work.

Acknowledgements

This work was funded by the European Research Council (ERC Grant Agreement 646747) and the Deutsche Forschungsgemeinschaft (DFG, 389479699/RTG2455). Quantum-chemical calculations of the Frankfurt group were performed at the Center for Scientific Computing (CSC) Frankfurt on the LOEWE-CSC computer cluster

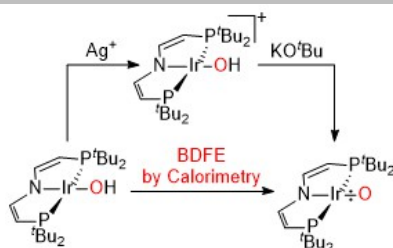
Keywords: Oxo Complex • Hydrogen Atom Transfer • Iridium • Pincer Complex

- [1] (a) C. Krebs, D. G. Fujimori, C. T. Walsh, J. M. Bollinger, *Acc. Chem. Res.* **2007**, 40, 484. (b) K. Gunay, A.; Theopold, *Chem. Rev.* **2010**, 1060.
- [2] (a) U. Hintermair, S. W. Sheehan, A. R. Parent, D. H. Ess, D. T. Richens, P. H. Vaccaro, G. W. Brudvig, R. H. Crabtree, *J. Am. Chem. Soc.* **2013**, 135, 10837. (b) M. Zhou, D. Balcells, A. R. Parent, R. H. Crabtree, O. Eisenstein, *ACS Catal.* **2012**, 2, 208.
- [3] M. C. Lehman, D. R. Pahls, J. M. Meredith, R. D. Sommer, D. M. Heinekey, T. R. Cundari, E. A. Ison, *J. Am. Chem. Soc.* **2015**, 137, 3574.
- [4] (a) J. Roizen, M. E. Harvey, J. Du Bois, *Acc. Chem. Res.* **2012**, 45, 911. (b) Y. Park, Y. Kim, S. Chang, *Chem. Rev.* **2017**, 117, 9247.
- [5] J. R. Winkler, H. B. Gray, *Struct. Bonding* **2012**, 142, 17.
- [6] Cobalt: (a) D. M. Jenkins, T. A. Betley, J. C. Peters, *J. Am. Chem.*

- Soc.* **2002**, 124, 11238. (b) X. Hu, K. Meyer, *J. Am. Chem. Soc.* **2004**, 126, 16322. (c) D. T. Shay, G. P. A. Yap, L. N. Zakharov, A. L. Rheingold, K. H. Theopold, *Angew. Chem. Int. Ed.* **2005**, 44, 1508. (d) R. E. Cowley, R. P. Bontchev, J. Sorrell, O. Sarracino, Y. Feng, H. Wang, J. M. Smith, *J. Am. Chem. Soc.* **2007**, 129, 2424. (e) J. Du, L. Wang, M. Xie, L. Deng, *Angew. Chem. Int. Ed.* **2015**, 54, 12640. (f) M. K. Goetz, E. A. Hill, A. S. Filatov, J. S. Anderson, *J. Am. Chem. Soc.* **2018**, 140, 13176. (g) M. K. Goetz, J. S. Anderson, *J. Am. Chem. Soc.* **2019**, 141, 4051. (h) Y. Liu, J. Du, L. Deng, *Inorg. Chem.* **2017**, 56, 8278.
- [7] Rhodium: A. M. Geer, C. Tejel, J. A. López, M. A. Ciriano, *Angew. Chemie - Int. Ed.* **2014**, 53, 5614.
- [8] Iridium: (a) D. S. Glueck, J. Wu, F. J. Hollander, R. G. Bergman, *J. Am. Chem. Soc.* **1991**, 113, 2041–2054. (b) R. S. Hay-Motherwell, G.

-
- Wilkinson, B. Hussain-Bates, M. B. Hursthouse, *Polyhedron* **1993**, 12, 2009.
- [9] (a) E. Poverenov, I. Efremenko, A. I. Frenkel, Y. Ben-David, L. J. W. Shimon, G. Leitus, L. Konstantinovski, J. M. L. Martin, D. Milstein, *Nature* **2008**, 455, 1093. (b) A. Grünwald, N. Orth, A. Scheurer, F. W. Heinemann, A. Pöthig, D. Munz, *Angew. Chem. Int. Ed.* **2018**, 57, 16228.
- [10] (a) D. J. Mindiola, G. L. Hillhouse, *J. Am. Chem. Soc.* **2001**, 123, 4623. (b) V. M. Iluc, G. Hillhouse, *J. Am. Chem. Soc.* **2010**, 132, 15148. (c) C. A. Laskowski, A. J. M. Miller, G. L. Hillhouse, T. R. Cundari, *J. Am. Chem. Soc.* **2011**, 133, 771.
- [11] (a) C. Limberg, *Angew. Chem. Int. Ed.* **2009**, 48, 2270. (b) D. Munz, *Chem. Sci.* **2018**, 9, 1155.
- [12] M. G. Scheibel, B. Askevold, F. W. Heinemann, E. J. Reijerse, B. de Bruin and S. Schneider, *Nat. Chem.* **2012**, 4, 552.
- [13] M. Kinauer, M. Diefenbach, H. Bamberger, S. Demeshko, E. J. Reijerse, C. Volkmann, C. Würtele, J. Van Slageren, B. De Bruin, M. C. Holthausen, S. Schneider, *Chem. Sci.* **2018**, 9, 4325.
- [14] J. Meiners, M. G. Scheibel, M. H. Lemée-Cailleau, S. A. Mason, M. B. Boeddinghaus, T. F. Fässler, E. Herdtweck, M. M. Khusniyarov, S. Schneider, *Angew. Chem. Int. Ed.* **2011**, 50, 8184.
- [15] For synthetic, spectroscopic, electrochemical, crystallographic and computational details see Electronic Supporting information.
- [16] (a) R. C. Stevens, R. Bau, *J. Chem. Soc. Dalton. Trans.* **1990** 1429. (b) D. Morales-Morales, D. W. Lee, Z. Wang, C. M. Jensen, *Organometallics* **2001**, 20, 1144. (c) R. J. Burford, W. E. Piers, D. H. Ess, M. Parvez, *J. Am. Chem. Soc.* **2014**, 136, 3256.
- [17] Note that the spin-Hamiltonian formalism loses its physical meaning in such cases of large spin-orbit coupling that mixes excited states into the ground state (see ref. 18a).
- [18] (a) M. Atanasov, D. Aravena, E. Suturina, E. Bill, D. Maganas, F. Neese, *Coord. Chem. Rev.* **2015**, 289, 177. (b) S. Kumar Singh, J. Eng, M. Atanasov, F. Neese, *Coord. Chem. Rev.* **2017**, 344, 2.
- [19] CCSD(T)-F12/VTZ:B3LYP(V)-D3/def2-TZVP ONIOM calculations based on a methyl truncated model, see Supporting Information.
- [20] M. Kinauer, M. G. Scheibel, J. Abbenseth, F. W. Heinemann, P. Stollberg, C. Würtele, S. Schneider, *Dalt. Trans.* **2014**, 43, 4506.
- [21] J. Abbenseth, D. Delony, M. C. Neben, C. Würtele, B. de Bruin, S. Schneider, *Angew. Chem. Int. Ed.* **2019**, DOI: 10.1002/anie.201901470.
- [22] Differential entropic contributions computed for reaction 1 at the B3LYP(V)-D3/def2TZVP level amount to $-8.2 \text{ J}\cdot\text{mol}^{-1}\cdot\text{K}^{-1}$.
- [23] (a) E. A. Mader, V. W. Manner, T. F. Markle, A. Wu, J. A. Franz, J. M. Mayer, *J. Am. Chem. Soc.* **2009**, 131, 4335. (b) V. W. Manner, A. D. Lindsay, E. A. Mader, J. N. Harvey, J. M. Mayer, *Chem. Sci.* **2012**, 3, 230.
- [24] C. Heinemann, H. Schwarz, W. Koch, K.G. Dyall, *J. Chem. Phys.* **1996**, 104, 4642.
- [25] (a) P. E. M. Siegbahn, M. Svensson, R. H. Crabtree, *J. Am. Chem. Soc.* **1995**, 117, 6758. (b) J. J. Carroll, J. C. Weisshaar, P. E. M. Siegbahn, C. A. M. Wittborn, M. R. A. Blomberg, *J. Phys. Chem. A* **1995**, 99, 14388. (c) K. Chen, G. Zhang, H. Chen, J. Yao, D. Danovich, S. Shaik, *J. Chem. Theory Comput.* **2012**, 8, 1641.
-

A terminal iridium(III) oxo complex was isolated and fully characterized. The ambiphilic oxo complex exhibits an unprecedented triplet ground state and large oxygen radical character. Thermochemical examination of the corresponding hydroxo/oxo ($\text{Ir}^{\text{III}}\text{OH}/\text{Ir}^{\text{IV}}\text{O}$) hydrogen atom transfer couple indicates that the O–H BD(F)E is sufficient for the activation of strong E–H bonds.



Daniel Delony, Markus Kinauer, Martin Diefenbach, Christian Würtele, Max Holthausen*, Sven Schneider*

Page No. – Page No.

A Terminal Iridium Oxo Complex with a Triplet Ground State